binds to the C terminus (*19*). In addition to these protein interactions, methylation of Lys[9] of histone H3 creates a high-affinity binding site for HP1, providing a mechanism for localization of this protein to RE-1 elements (*20*, *21*). Our study identifies SCPs as functional components of the REST/NRSF silencing complex (Fig. 4B). The negative influence of SCPs on the transcription of neuronal genes may be mediated by dephosphorylation of the CTD of RNAPII; it is possible, however, that other phosphatase substrates mediate these effects (*22*). Moreover, other related phosphatases with the DXDX(T/V) amino acid signature found in FCP1-class proteins might contribute to gene regulation by using similar mechanisms. For example, the eyes absent (Eya) transcription cofactor is a protein phosphatase belonging to this general family that serves to convert the DNA binding homeodomain protein sine oculis from a repressor to an activator, promoting eye formation in *Drosophila* and cell proliferation required for organ formation in mice (kidney and muscle) (*23*, *24*). In addition, SCP2 is reported to dorsalize the ventral mesoderm, indicating it might also help to negatively regulate a subset of non-neuronal genes (*25*).

These data provide further evidence that a variety of mechanisms are used by REST/NRSF to suppress neuronal gene expression. Previous studies have focused on interactions with deacetylases and methylases that modify chromatin (Fig. 4B). Here we show that a mechanism involving SCPs also contributes to blocking inappropriate neuronal gene expression in developing cells. The mechanisms that inhibit the expression of any particular gene are likely to vary considerably, but our findings suggest that antagonism of the SCP pathway might help to promote neuronal differentiation from the appropriate cell types.

References and Notes

1. J. A. Chong *et al.*, *Cell* **80**, 949 (1995).
2. C. J. Schoenherr, D. J. Anderson, *Science* **267**, 1360 (1995).
3. Z. F. Chen, A. J. Paquette, D. J. Anderson, *Nature Genet.* **20**, 136 (1998).
4. M. A. Hakimi *et al.*, *Proc. Natl. Acad. Sci. U.S.A.* **99**, 7420 (2002).
5. Y. Naruse, T. Aoki, T. Kojima, N. Mori, *Proc. Natl. Acad. Sci. U.S.A.* **96**, 13691 (1999).
6. K. Kokura *et al.*, *J. Biol. Chem.* **276**, 34115 (2001).
7. M. Yeo, P. S. Lin, M. E. Dahmus, G. N. Gill, *J. Biol. Chem.* **278**, 26078 (2003).
8. T. Kamenski, S. Heilmeier, A. Meinhart, P. Cramer, *Mol. Cell* **15**, 399 (2004).
9. V. V. Lunyak *et al.*, *Science* **298**, 1747 (2002).
10. M. Yeo *et al.*, data not shown.
11. A. Roopra *et al.*, *Mol. Cell. Biol.* **20**, 2147 (2000).
12. M. Yao, G. Bain, D. I. Gottlieb, *J. Neurosci. Res.* **41**, 792 (1995).
13. Q. Ma, C. Kintner, D. J. Anderson, *Cell* **87**, 43 (1996).
14. S. K. Lee, S. L. Pfaff, *Neuron* **38**, 731 (2003).
15. G. Bai, Z. Zhuang, A. Liu, Y. Chai, P. W. Hoffman, *J. Neurochem.* **86**, 992 (2003).
16. The gene expression database of the Berkeley Drosophila Genome Project is available at: www.fruitfly.org/cgi-bin/ex/bquery.pl?qtype=report&find=CG5830&searchfield=CG.
17. M. R. Freeman, J. Delrow, J. Kim, E. Johnson, C. Q. Doe, *Neuron* **38**, 567 (2003).
18. C. J. Schoenherr, A. J. Paquette, D. J. Anderson, *Proc. Natl. Acad. Sci. U.S.A.* **93**, 9881 (1996).
19. M. E. Andres *et al.*, *Proc. Natl. Acad. Sci. U.S.A.* **96**, 9873 (1999).
20. M. Lachner, D. O'Carroll, S. Rea, K. Mechtler, T. Jenuwein, *Nature* **410**, 116 (2001).
21. A. J. Bannister *et al.*, *Nature* **410**, 120 (2001).
22. T. Maile *et al.*, *Science* **304**, 1010 (2004).
23. T. L. Tootle *et al.*, *Nature* **426**, 299 (2003).
24. X. Li *et al.*, *Nature* **426**, 247 (2003).
25. I. E. Zohn, A. H. Brivanlou, *Dev. Biol.* **239**, 118 (2001).

26. The authors are grateful to V. Lunyak and I. Kalcheva for helpful advice. S.-K.L. was supported by a fellowship from the Human Frontiers Science Program, and S.L.P was supported by the Helen McLoraine Developmental Chair in Neurobiology and the G. Harold and Leila Y. Mathers Foundation. These studies were supported by NIH grant DK13149 (G.N.G.) and NS37116 (S.L.P.).

Supporting Online Material

www.sciencemag.org/cgi/content/full/307/5709/596/DC1
Materials and Methods
Figs. S1 to S3

27 May 2004; accepted 1 December 2004
10.1126/science.1100801

Illumination of the Melanopsin Signaling Pathway

Satchidananda Panda,*†‡ Surendra K. Nayak,* Brice Campo, John R. Walker, John B. Hogenesch,§ Tim Jegla†

In mammals, a small population of intrinsically photosensitive retinal ganglion cells (ipRGCs) plays a key role in the regulation of nonvisual photic responses, such as behavioral responses to light, pineal melatonin synthesis, pupillary light reflex, and sleep latency. These ipRGCs also express melanopsin (Opn4), a putative opsin-family photopigment that has been shown to play a role in mediating these nonvisual photic responses. Melanopsin is required for the function of this inner retinal pathway, but its precise role in generating photic responses has not yet been determined. We found that expression of melanopsin in *Xenopus* oocytes results in light-dependent activation of membrane currents through the $G\alpha_q/G\alpha_{11}$ G protein pathway, with an action spectrum closely matching that of melanopsin-expressing ipRGCs and of behavioral responses to light in mice lacking rods and cones. When coexpressed with arrestins, melanopsin could use all-*trans*-retinaldehyde as a chromophore, which suggests that it may function as a bireactive opsin. We also found that melanopsin could activate the cation channel TRPC3, a mammalian homolog of the *Drosophila* phototransduction channels TRP and TRPL. Melanopsin therefore signals more like an invertebrate opsin than like a classical vertebrate rod-and-cone opsin.

Nonvisual photoresponses in mammals, including circadian entrainment, constriction of the pupil, and regulation of sleep latency, are generated in part by a network of ipRGCs that directly innervate the brain regions that mediate these responses (*1*–*7*). The photosensitivity of these cells is dependent on melanopsin (Opn4) (*2*, *5*, *6*), an atypical vertebrate opsin first isolated from frog melanophores (*8*). Genetic studies have indicated that nonvisual responses to light persist in mice lacking rod and cone function but are entirely eliminated if melanopsin is also removed (*9*, *10*). Although these studies have established the critical role of melanopsin in photosensation within the inner retina, the underlying mechanism has remained uncharacterized.

Vertebrate and invertebrate photosensitive opsins are heterotrimeric guanine nucleotide–binding protein (G protein)–coupled receptors that use 11-*cis*-retinaldehyde (11-*cis*-retinal) or a close variant as their chromophore (*11*). Photoconversion of the 11-*cis*-retinal to all-*trans*-retinaldehyde (all-*trans*-retinal) creates a conformational change in these opsin proteins that triggers G protein activation and subsequent signaling. Vertebrate rod-and-cone opsins signal through photoreceptor-specific, pertussis toxin (PTX)–sensitive G proteins called transducins, whereas invertebrate opsins signal through the PTX-insensitive G_q family of G proteins (*11*). These responses are terminated by a combination of phosphorylation of the excited opsin and the binding of arrestin proteins (*12*). After signaling, re-

Genomics Institute of Novartis Research Foundation, 10675 John J. Hopkins Drive, San Diego, CA 92121, USA.

*These authors contributed equally to this work.
†To whom correspondence should be addressed. E-mail: satchin@salk.edu, tjegla@gnf.org
‡Present address: Salk Institute for Biological Studies, La Jolla, CA 92037, USA.
§Present address: Scripps Florida, FAU-Building MC-17, 5353 Parkside Drive, Jupiter, FL 33458, USA.

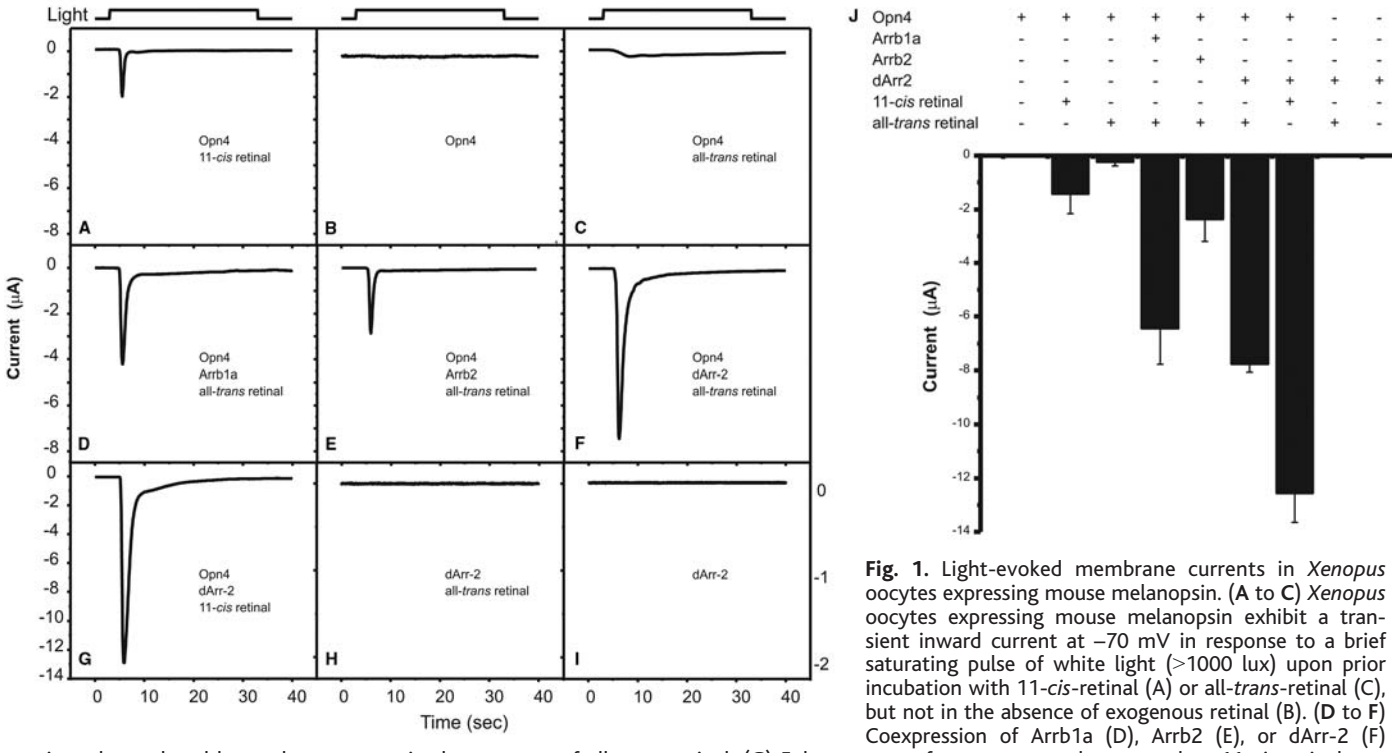

Fig. 1. Light-evoked membrane currents in *Xenopus* oocytes expressing mouse melanopsin. (**A** to **C**) *Xenopus* oocytes expressing mouse melanopsin exhibit a transient inward current at –70 mV in response to a brief saturating pulse of white light (>1000 lux) upon prior incubation with 11-*cis*-retinal (A) or all-*trans*-retinal (C), but not in the absence of exogenous retinal (B). (**D** to **F**) Coexpression of Arrb1a (D), Arrb2 (E), or dArr-2 (F) consistently produced large photocurrents in the presence of all-*trans*-retinal. (**G**) Enhancement of currents was also seen when 11-*cis*-retinal was used as the chromophore. (**H** and **I**) Oocytes injected with arrestin alone did not produce a photocurrent in the presence (H) or absence (I) of all-*trans*-retinal. (**J**) Mean peak photocurrent (±SEM, n = 3 to 9 oocytes) from oocytes under different conditions of mRNA and chromophore. All recordings were made under voltage clamp at –70 mV; see (*20*) for details of chromophore incubation and light application.

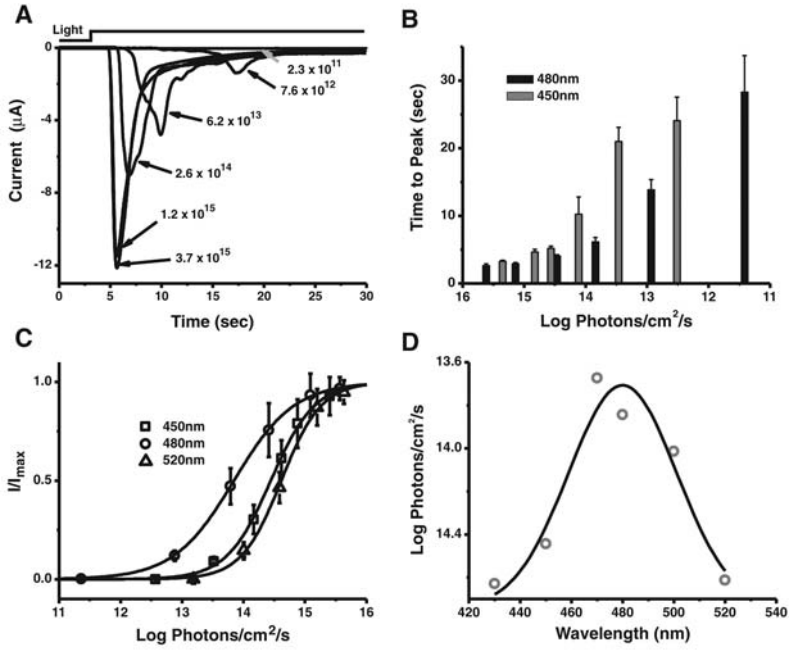

Fig. 2. Spectral sensitivity of melanopsin-mediated photocurrent. Photocurrents were generated from oocytes injected with mouse melanopsin and dArr-2 in response to light pulses of varying wavelength and intensity after exposure to 11-*cis*-retinal (*20*). (**A**) Representative photocurrents elicited in response to 40-s pulses of 480-nm light of varying intensity. Light pulse duration is indicated at the top with a bar; light intensity for each trace is given in photons cm^{-2} s^{-1}. Voltage was held at –70 mV for all recordings. The size and speed of the response correlate well with light intensity. (**B**) Mean time lag (±SEM; $n \geq 5$) from onset of the light pulse to peak of the photocurrent for pulses of 450-nm and 480-nm light of varying intensity. The time lag increases with decreasing light intensity at both wavelengths. The lag is shorter at intermediate intensities for 480-nm light, which suggests that it is more effective in eliciting the photoresponse. (**C**) Normalized irradiance-response curves for light wavelengths of 450, 480, and 520 nm. Bars indicate SE (n = 4 to 8); lines show sigmoidal fits of the data. Note the higher sensitivity of the response to 480-nm light. (**D**) Half-activation values, derived from sigmoidal fits of irradiance-response curves, plotted versus wavelength and fit with a Gaussian function (peak amplitude = 479.8 nm).

generation of the active chromophore is necessary to restore photosensitivity. In vertebrates, this process involves release of all-*trans*-retinal from the opsin and conversion back to 11-*cis*-retinal through an elaborate pathway resident primarily in the retinal pigment epithelium. Invertebrate opsins, such as *Drosophila* rhodopsin 1, instead photoconvert all-*trans*-retinal back to the active form in an arrestin-dependent manner (*13*) and therefore also function as photoisomerases, obviating the need for an accessory pigment regeneration mechanism. Sequence comparisons have shown that melanopsin shares significant similarity to opsins from invertebrates (*8*), and therefore melanopsin may function more like an invertebrate opsin than like vertebrate rod-and-cone opsins. Interestingly, both melanopsin-containing *Xenopus* melanophores (*14*) and ipRGCs from rodents (*5*) exhibit photosensitivity that persists ex vivo in the presence of all-*trans*-retinal, supporting this notion.

To characterize light-dependent melanopsin function, we injected mRNA encod-

ing mouse melanopsin into *Xenopus* oocytes and recorded whole-cell currents elicited in response to light pulses after exposure of the oocytes to retinaldehyde-based chromophores. *Xenopus* oocytes have been successfully used to express and functionally characterize opsins in a wide range of organisms, including bacteria and mammals (*15*–*19*). Melanopsin-expressing oocytes incubated with 11-*cis*-retinal (*20*) produced large, transient currents in response to illumination with saturating bright white light (>1000 lux) (Fig. 1A). Photocurrents were not observed in the absence of 11-*cis*-retinal (Fig. 1B) or in uninjected oocytes incubated with 11-*cis*-retinal (*21*). These results clearly indicate that melanopsin is a functional photoreceptive opsin capable of using 11-*cis*-retinal as a chromophore. Incubation of injected oocytes with all-*trans*-retinal led to small photocurrents observed in a subset of oocytes (Fig. 1C). Photoconversion of all-*trans*-retinal to the active 11-*cis* conformation is arrestin-dependent in invertebrates (*13*), and *Drosophila* rhodopsin 1/all-*trans*-retinal–based photocurrents in oocytes are dependent on coexpression of an arrestin (*19*). Thus, we reasoned that the difficulty in eliciting consistent photoresponses from oocytes incubated with all-*trans*-retinal could be corrected by coexpression of melanopsin with an arrestin. Indeed, we found that coexpression of melanopsin with mouse β1 arrestin (Arrb1a, GenBank accession number NM_177231), mouse β2 arrestin (Arrb2, GenBank accession number NM_145429), or fly arrestin-2 (dArr-2, GenBank accession number M32141) resulted in large, consistent photocurrents from eggs incubated with all-*trans*-retinal (Fig. 1, D, E, F, and J). The magnitude of photocurrents was also enhanced by arrestins when 11-*cis*-retinal was used as a chromophore (Fig. 1, G and J). Arrestin alone did not produce a light response (Fig. 1, H to J), thereby ruling out the possibility that the increased photosensitivity is due to coupling of arrestin to an endogenous photoreceptor. Together these observations show that melanopsin is a true photosensory opsin and that, like invertebrate opsins, it may be able to complete the retinoid cycle through intrinsic photoisomerase activity.

We next generated an action spectrum of the melanopsin-mediated photocurrent in oocytes to test whether the responses faithfully reproduced the spectral sensitivity of ipRGCs and the inner retinal nonvisual photopathway. Peak responsiveness is found at a light wavelength of about 480 nm for the excitation of ipRGCs (*5*) as well as for circadian entrainment (*6*, *22*) and pupillary constriction (*23*) responses mediated by the inner retina pathway. We measured the irradiance-response relationship for the photocurrent at near-monochromatic light (half peak bandwidth = 10 nm) of different wavelengths from oocytes expressing both melanopsin and arrestin (*20*). Reduction in light intensity led to both a reduction in the peak of the photocurrent and a delay in the onset (Fig. 2, A to C). The irradiance for half-maximal photocurrent at each wavelength was plotted to generate an action spectrum (Fig. 2D). The spectrum clearly peaks between 460 and 480 nm, and is best fitted by a Gaussian function with a peak of 480 nm ($r^2 = 0.925$). Thus, the spectral properties of melanopsin in oocytes are highly consistent with the observed function of ipRGCs. However, the absorption spectrum of in vitro reconstituted melanopsin purified from cultured mammalian cells exhibits a peak absorbance in the 420- to 440-nm range (*24*). Cell-specific factors and/or the protein purification procedure may influence the spectral properties of the chromophore and hence may underlie this discrepancy.

We next examined the relevant G protein signaling pathway used by melanopsin to produce the observed photocurrent in oocytes. We reasoned that activation of the well-characterized native oocyte calcium-activated chloride current was largely responsible for

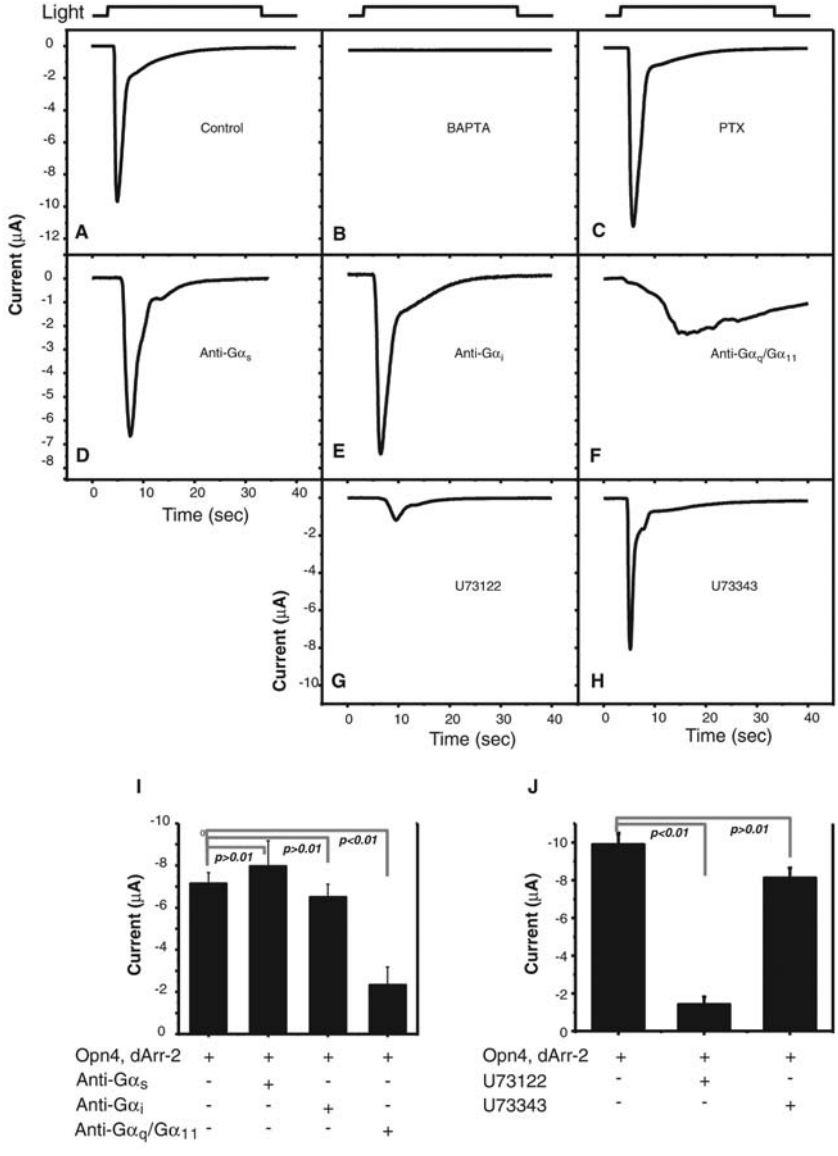

Fig. 3. Role of $G\alpha_q/G\alpha_{11}$ and PLC in generating melanopsin-dependent photocurrents. (**A**) A typical melanopsin-mediated photocurrent recorded in response to light (white, >1000 lux) after incubation with all-*trans*-retinal. (**B** and **C**) The photocurrent is abolished in oocytes injected with 50 nl of BAPTA (50 mM) (B) but is unaffected by injection of 50 nl of PTX (1 ng/μl) (C). (**D** and **E**) The photocurrent could not be blocked by injection of 50 nl of antibodies to $G\alpha_s$ (D) or $G\alpha_i$ (E) classes of G proteins. (**F**) Injection of antibodies recognizing a common epitope in both $G\alpha_q$ and $G\alpha_{11}$ severely attenuated the photocurrent. (**G**) Incubation of the oocytes with the PLC inhibitor U73122 (1 μM) attenuated the photocurrent. (**H**) Incubation in solution containing an inactive analog U73343 (1 μM) had little effect. (**I**) and (**J**) Mean values (±SEM, n = 4 to 8 oocytes) for antibody and PLC inhibitor experiments, respectively. Significance of difference was tested by Student's t test (equal variance); the corresponding P values are indicated. See (*20*) for details of methods.

the photocurrent, because the current reversed close to the predicted equilibrium potential for chloride and was reduced by known blockers of this channel (*21*). Injection of oocytes with the calcium chelator 1,2-bis(2-aminophenoxy)ethane-*N*,*N*,*N*′,*N*′-tetraacetic acid (BAPTA) before recording eliminated the bulk of the photocurrent; this result further suggested that a rise in intracellular calcium is the trigger for the photocurrent we observed in oocytes (Fig. 3B). This response was insensitive to injection of PTX (Fig. 3C), which blocks transduction through $G_i/G_o/G_t$ class G proteins. In contrast, PTX was highly effective in blocking the potentiation of GIRK currents by the G_i-coupled M2 muscarinic receptor in the oocyte system (*21*). Taken together, these results imply the involvement of G_q/G_{11} class G proteins, which are the classic activators of phospholipase C–β (PLC-β). Activated PLC breaks down phosphatidylinositol 4,5-bisphosphate to inositol 1,4,5-trisphosphate and diacylglycerol (DAG), and also triggers calcium release from intracellular stores.

We found that we could block the melanopsin-induced photocurrent with injection of antibodies to $G\alpha_q/G\alpha_{11}$, but not with antibodies to $G\alpha_s$ or $G\alpha_i$ (Fig. 3, D, E, F, and I). In addition, the PLC inhibitor U73122, but not its inactive analog U73343, was highly effective in blocking the photocurrent (Fig. 3, G, H, and J). Although we cannot rule out association of melanopsin with other G proteins under special circumstances, as has been previously shown (*24*), our results clearly point to a model whereby light-activated melanopsin preferentially activates the G_q/G_{11} class of G proteins, followed by activation of PLC-β.

Because this signaling mechanism is similar to that used by invertebrate opsins, we reasoned that mammalian transient receptor potential (TRP) subfamily C (TRPC) cation channels, which are paralogs of the *Drosophila* phototransduction channels Trp and Trpl (*25*, *26*), could be involved in phototransduction in ipRGCs. Although the molecular identity of the phototransduction channel(s) in ipRGCs remains unknown, excitation of ipRGCs by light leads to both calcium influx and depolarization (*5*, *27*, *28*), as is observed in *Drosophila* photoreceptors. The current-voltage relationship of light-activated current in ipRGCs is similar to that of the TRP class of channels, in that it shows a reversal potential indicative of a nonselective cation channel and displays outward rectification at depolarized voltages (*28*). In addition, TRPC channels are calcium-permeable nonselective cation channels and are activated by the G_q/G_{11} pathway (*29*). To test this hypothesis, we coexpressed melanopsin with mouse TRPC3 in oocytes. TRPC3 produced a novel sustained component in photocurrents that could be partially blocked with 1 mM lanthanum (La^{3+}), a known TRPC channel blocker (Fig. 4A). Injection of BAPTA before recording allowed the TRPC3 photocurrent to be observed in isolation from the transient native calcium-activated chloride currents (Fig. 4B). Insensitivity of the TRPC-based photocurrent to calcium chelation suggests activation via DAG, as has been observed for mammalian TRPC channels, including TRPC3 (*29*). The photocurrent was also attenuated upon prior incubation of the oocytes with U73122 (65.4% attenuation in the presence of U73122, n = 8). The isolated melanopsin-dependent TRPC3 photocurrents remained activated for the duration of light pulses, and they were completely blocked by La^{3+} or greatly reduced by replacement of extracellular sodium with *N*-methyl-D-glucamine (NMDG) (Fig. 4, B and C). Voltage ramps taken during light pulses show that the TRPC3 photocurrent has a profile similar to that of ipRGCs (*28*); it has a reversal potential typical of a nonselective cation channel and displays outward rectification at higher voltages (Fig. 4D). In the absence of arrestins, the TRPC3 photocurrent did not decrease after the end of the light pulse (Fig. 4E) and persisted for minutes (*21*) before returning to baseline. Therefore, arrestins may play an important role in terminating light-evoked melanopsin signaling, as they do for both invertebrate opsins and vertebrate rod-and-cone opsins. Differences in the amplitudes of TRPC3-mediated photocurrents with and without arrestin were most pronounced with multiple light pulses separated by several minutes. Responses to a second identical light pulse were greatly reduced in the absence of arrestin (26.2 ± 9.5% of initial response, n = 5). In contrast, second responses were potentiated in the presence of arrestin (195 ± 43% of initial response, n = 4), further suggesting the arrestin dependence of photoregeneration in melanopsin signaling. Although these observations do not constitute proof that TRPC family channels are involved in ipRGC phototransduction, members of this gene family can be considered prime candidates for the phototransduction channel of the inner retinal pathway in mammals. We were not able to demonstrate photoactivation of channels from the TRPV (TRPV1), TRPM (TRPM8), and TRPA (TRPA1) families in similar experiments (*21*).

Our results show that melanopsin encodes a fully functional opsin through its ability to confer photosensitivity to *Xenopus* oocytes. The action spectrum of the photocurrent closely matches that of photosensitivity of ipRGCs in

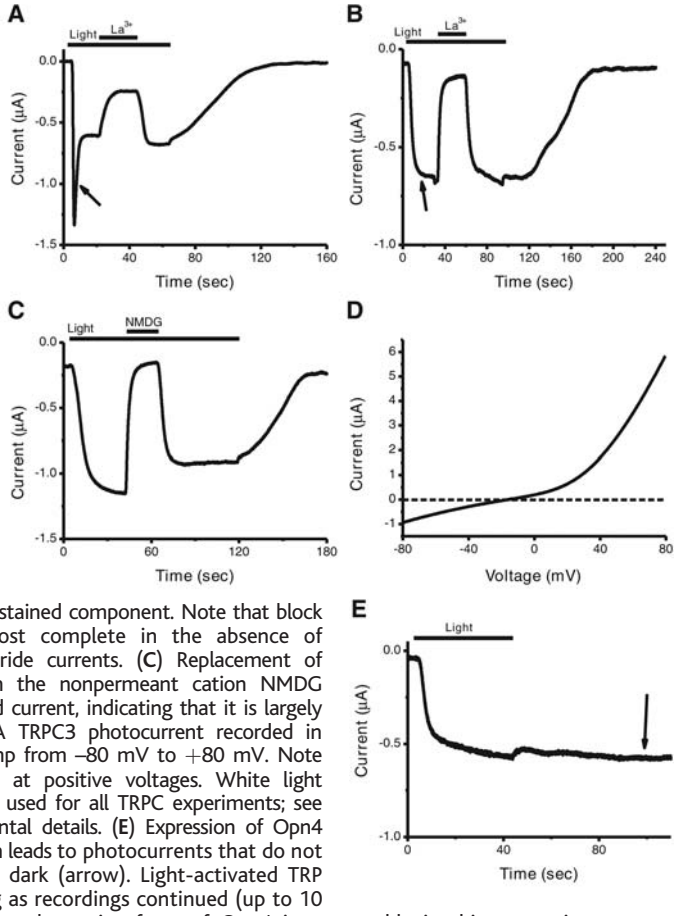

Fig. 4. Melanopsin activates TRPC channels in a light-dependent manner. (**A**) A photocurrent for a *Xenopus* oocyte expressing Opn4, dArr-2, and mouse TRPC3 shows the typical transient calcium-activated chloride current (arrow) but also contains a novel sustained component that is partially blocked by 1 mM lanthanum (La^{3+}) (bar). The current slowly returns to baseline after light is turned off. (**B**) Injection of oocytes expressing Opn4, dArr-2, and TRPC3 with 50 nl of 50 mM BAPTA before recording abolishes the calcium-activated chloride current (arrow) but does not affect the sustained component. Note that block by 1 mM La^{3+} is almost complete in the absence of contamination from chloride currents. (**C**) Replacement of extracellular sodium with the nonpermeant cation NMDG greatly reduces the inward current, indicating that it is largely carried by sodium. (**D**) A TRPC3 photocurrent recorded in response to a voltage ramp from –80 mV to +80 mV. Note the outward rectification at positive voltages. White light pulses of >1000 lux were used for all TRPC experiments; see (*20*) for further experimental details. (**E**) Expression of Opn4 and TRPC3 without arrestin leads to photocurrents that do not return to baseline in the dark (arrow). Light-activated TRP currents persisted as long as recordings continued (up to 10 min), which indicates that the active form of Opn4 is very stable in this expression system. Voltage was held at –70 mV in (A), (B), (C), and (E).

rodents, which implies that melanopsin alone can account for the intrinsic photosensitivity of these RGCs. Furthermore, melanopsin functionally resembles invertebrate opsins in that it can activate both G_q/G_{11} signaling pathways and TRPC channels, and it appears to have an intrinsic photoisomerase activity. The photoisomerase activity of melanopsin may be particularly important for its function in ipRGCs because they are spatially distant from the retinal pigment epithelium, which participates in chromophore regeneration for rod-and-cone opsins. The genetic manipulation of proposed components of the signaling cascade expressed in melanopsin-containing ipRGCs will ultimately determine their role in melanopsin-based photic responses.

Note added in proof: Similar findings have recently been reported (*30*, *31*).

References and Notes

1. N. F. Ruby *et al.*, *Science* **298**, 2211 (2002).
2. S. Hattar, H. W. Liao, M. Takao, D. M. Berson, K. W. Yau, *Science* **295**, 1065 (2002).
3. J. Hannibal, P. Hindersson, S. M. Knudsen, B. Georg, J. Fahrenkrug, *J. Neurosci.* **22**, RC191 (2002).
4. J. J. Gooley, J. Lu, T. C. Chou, T. E. Scammell, C. B. Saper, *Nature Neurosci.* **4**, 1165 (2001).
5. D. M. Berson, F. A. Dunn, M. Takao, *Science* **295**, 1070 (2002).
6. R. J. Lucas *et al.*, *Science* **299**, 245 (2003).
7. S. Panda *et al.*, *Science* **298**, 2213 (2002).
8. I. Provencio, G. Jiang, W. J. De Grip, W. P. Hayes, M. D. Rollag, *Proc. Natl. Acad. Sci. U.S.A.* **95**, 340 (1998).
9. S. Panda *et al.*, *Science* **301**, 525 (2003).
10. S. Hattar *et al.*, *Nature* **424**, 76 (2003).
11. R. C. Hardie, P. Raghu, *Nature* **413**, 186 (2001).
12. M. E. Burns, D. A. Baylor, *Annu. Rev. Neurosci.* **24**, 779 (2001).
13. A. Kiselev, S. Subramaniam, *Biochemistry* **36**, 2188 (1997).
14. M. D. Rollag, I. Provencio, D. Sugden, C. B. Green, *Methods Enzymol.* **316**, 291 (2000).
15. G. Nagel *et al.*, *Proc. Natl. Acad. Sci. U.S.A.* **100**, 13940 (2003).
16. G. Nagel *et al.*, *Science* **296**, 2395 (2002).
17. H. G. Khorana, B. E. Knox, E. Nasi, R. Swanson, D. A. Thompson, *Proc. Natl. Acad. Sci. U.S.A.* **85**, 7917 (1988).
18. B. E. Knox, R. B. Barlow, D. A. Thompson, R. Swanson, E. Nasi, *Methods Enzymol.* **316**, 41 (2000).
19. B. V. Zemelman, G. A. Lee, M. Ng, G. Miesenbock, *Neuron* **33**, 15 (2002).
20. See supporting data on *Science* Online.
21. S. Panda *et al.*, data not shown.
22. J. S. Takahashi, P. J. DeCoursey, L. Bauman, M. Menaker, *Nature* **308**, 186 (1984).
23. R. J. Lucas, R. H. Douglas, R. G. Foster, *Nature Neurosci.* **4**, 621 (2001).
24. L. A. Newman, M. T. Walker, R. L. Brown, T. W. Cronin, P. R. Robinson, *Biochemistry* **42**, 12734 (2003).
25. C. Montell, G. M. Rubin, *Neuron* **2**, 1313 (1989).
26. A. M. Phillips, A. Bull, L. E. Kelly, *Neuron* **8**, 631 (1992).
27. S. Sekaran, R. G. Foster, R. J. Lucas, M. W. Hankins, *Curr. Biol.* **13**, 1290 (2003).
28. E. J. Warren, C. N. Allen, R. L. Brown, D. W. Robinson, *Eur. J. Neurosci.* **17**, 1727 (2003).
29. M. Trebak, G. Vazquez, G. S. Bird, J. W. Putney Jr., *Cell Calcium* **33**, 451 (2003).
30. Z. Meylan *et al.*, *Nature*, in press; published online 26 January 2005 (10.1038/nature03344).
31. X. Qiu *et al.*, *Nature*, in press; published online 26 January 2005 (10.1038/nature03345).

32. Supported by the Novartis Research Foundation. We thank A. Patapoutian for the TRPC3 clone, R. Crouch for 11-*cis*-retinal, and K. Naik, V. Lee, and V. Piamonte for expert technical assistance.

Supporting Online Material

www.sciencemag.org/cgi/content/full/307/5709/600/DC1
Materials and Methods
References

10 September 2004; accepted 23 November 2004
10.1126/science.1105121